Improving the sensitivity of scanning probe microscopy with mechanical vibrations

Eylon Persky, Naor Vardi, Yishai Shperber, and Beena Kalisky[a)]
Department of Physics and Institute of Nanotechnology and Advanced Materials, Bar-Ilan University, Ramat Gan 5290002, Israel

(Received 10 August 2018; accepted 5 October 2018; published online 22 October 2018)

Mechanical vibrations are typically undesired in imaging systems, as they cause noise and hinder system performance. Here, we propose to use vibrations in order to improve the sensitivity of a scanning probe system. We model the spectral and spatial structures of the response to an induced vibration and test our calculation on magnetic objects using a scanning superconducting quantum interference device microscope. In our experiments, we show that imaging the response to vibrations enhances the sensitivity of our sensor, as we detect signals that would otherwise be below the sensor's low frequency noise limit. Our results open the door to an effective way of improving the performance of many imaging systems. https://doi.org/10.1063/1.5051620

The low frequency noise spectrum of many sensors is dominated by 1/f noise. Therefore, it is often desirable to conduct measurements at higher frequencies, where the sensor reaches its noise floor. When one is interested in probing the sample's response to an applied field, it is easy to overcome the 1/f noise by using a lock-in technique: introducing AC excitations with specified frequencies to the sample and reading the sample's response. This technique is used, for example, to measure magnetic susceptibility (response to an external magnetic field) and dielectric constant (response to an external electric field).[1,2]

When the measured DC field is position dependent, it is possible to make the measured signal time dependent by varying the position of the sample with time, i.e., by vibrating the sample with respect to the sensor. This method is used in several bulk measurement systems, such as vibrating sample magnetometers.[3]

While commonly used to increase the sensitivity of bulk measurement systems, the use of vibrations in microscopy techniques is limited. Ideally, vibrations are avoided, unless they are essential to the sensor's readout, as is the case in the cantilever vibrations in force microscopy.[4,5] Here, we propose a general measurement scheme that utilizes controlled mechanical vibrations to increase the sensitivity of an imaging system. We study the spatial and spectral effects of vibrations, apply this method to scanning superconducting quantum interference device (SQUID) microscopy, and demonstrate its capabilities.

SQUID is a highly sensitive magnetometer, based on a superconducting loop with two Josephson junctions.[6,7] Our sensors are designed for scanning, with a detection loop fabricated near the edge of a silicon chip.[8–11] The sensors we use here have a detection loop with a diameter of 1 μm and maintain a flux sensitivity of $1\mu\Phi_0$ ($\Phi_0 = h/2e$ is the magnetic flux quantum). Magnetic field images are obtained by rastering the sample relative to the SQUID, using piezoelectric s-benders. The scanner [schematically drawn in Fig. 1(a)] allows a 500 μm square scan range, while enabling nanometric control over the sample's position.[12] Coarse motion is performed by a stick-slip motion system. The microscope can be loaded into a liquid helium dewar, or into a closed-cycle cooling system. Most of the experiments described here were performed in a closed-cycle system. Closed-cycle systems enable longer measurement times, at a lower cost of operation, compared to a liquid helium based system. However, the increased electrical noise and vibrations in this system hinder the SQUID's performance.[13] These effects are most severe at low frequencies ($<$100 Hz), since the operation of the cryo-cooler is in this frequency regime. This makes utilizing vibrations in such systems even more beneficial.

The spatial and spectral responses of the signal to an oscillation in the sample's position are encompassed in a simple, general model: suppose the sample's surface is located at the x-y plane. The SQUID measures the out-of-plane component of the magnetic field, $B_z(\mathbf{r})$, where $\mathbf{r} = (x, y)$ is the position of the sensor relative to the origin, and the sensor is located at some plane $z = z_0$. We apply an oscillatory voltage with a small amplitude x_0 and a frequency ω_0, to the x piezo elements, making the sample vibrate: $x(t) = x(t = 0) + x_0 \cos \omega_0 t$. The magnetic field is now time dependent through the position, $B_z(\mathbf{r}, t) = B_z(\mathbf{r}(t))$.

A function $f(\mathbf{r}, t)$ may be decomposed into its Fourier components according to

$$f(\mathbf{r},t) = \frac{1}{(2\pi)^3}\int dx dy dt \exp\left(i\mathbf{k}\cdot\mathbf{r} + i\omega t\right) f(\mathbf{k},\omega). \quad (1)$$

We may decompose $B_z(\mathbf{r}, t)$ into its Fourier components. Performing the integration over x and y, we have

$$B_z(\mathbf{k},\omega) = \int dt \exp\left(-i\omega t - ik_x x_0 \cos\omega_0 t\right) B_z(\mathbf{k},0). \quad (2)$$

We expand the exponent $\exp\left(-ik_x x_0 \sin\omega_0 t\right)$ to its Taylor series

[a)]beena@biu.ac.il

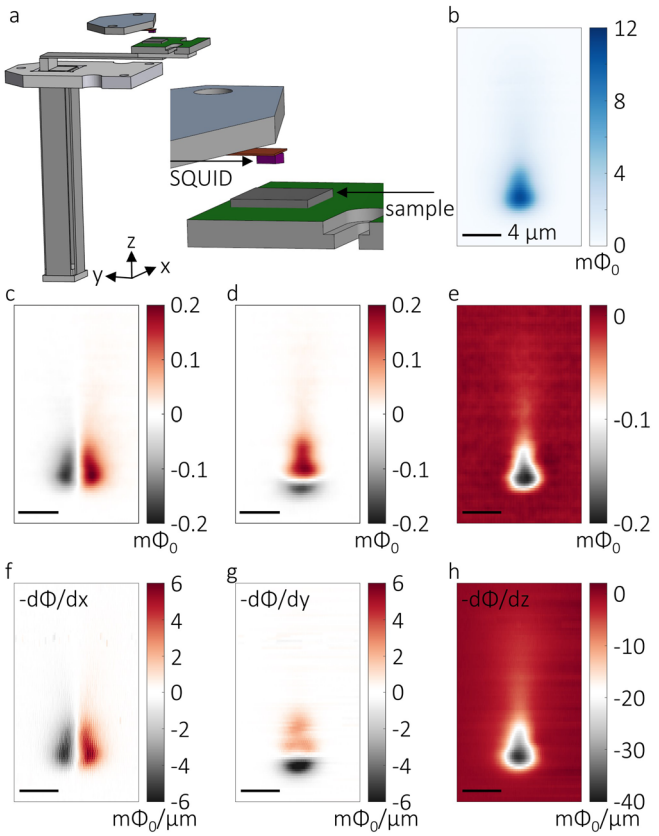

FIG. 1. Imaging response to vibrations. (a) A scheme of the SQUID microscope. The sample is mounted on top of a piezo-based scanner, and the sensor hovers above the sample. Scanning is achieved by varying the voltage applied to the piezo elements (gray) and vibrations are induced by adding an oscillatory voltage. (b) DC magnetic flux image of an isolated vortex in a 150 nm thick Nb film. (c)–(e) Signal measured in response to vibrations introduced in the x (c), y (d), and z (e) directions, at a frequency of 113 Hz. The vibration amplitude was 80 nm in x and y and 15 nm in z. (f)–(h) Derivatives of the data shown in panel (b) with respect to the x (f), y (g), and z (h) directions, demonstrating that the response to vibration has a spatial structure like the DC signal's gradient. Scale bar is 4 μm.

$$B_z(\mathbf{k},\omega) = B_z(\mathbf{k},t=0)\sum_{n=0}^{\infty}\left[\frac{1}{n!}(-ik_x x_0)^n \times \int dt \exp(-i\omega t)(\cos\omega_0 t)^n\right]. \quad (3)$$

Measuring the response at the vibration frequency is equivalent to evaluating the integrals in Eq. (3) at $\omega = \omega_0$. For even n, these integrals vanish. Therefore, Eq. (3) takes the form

$$B_z(\mathbf{k},\omega_0) = B_z(\mathbf{k},t=0)\sum_{n=0}^{\infty} A_{2n+1}(-x_0 ik_x)^{2n+1}, \quad (4)$$

where A_{2n+1} are the results of the remaining integrals. For a small vibration amplitude, such that $k_x x_0 \ll 1$, we may neglect the high order terms $(n \geq 1)$ in the expansion and return to the real space representation

$$B_z(\mathbf{r},\omega=\omega_0) = -\frac{1}{2}x_0\frac{\partial}{\partial x}B_z(\mathbf{r};t=0). \quad (5)$$

Remarkably, the response to vibrations has a distinct spatial structure, different from the original, unperturbed DC signal. Namely, the signal should be spatially distributed like the original field's gradient.

Figure 1 shows representative experimental results demonstrating our method. We imaged the magnetic signal from an individual vortex in a 150 nm thick superconducting Nb film (the time dependence of the magnetic signal from a vortex was used to analyse sensor-sample vibrations in other work[14]). Figure 1(b) shows a 13 μm by 22 μm image of the DC magnetic flux generated by such a vortex, while Figs. 1(c)–1(e) show the signal resulting from vibrations induced at the x, y, z axes, respectively. The amplitude of the vibrations was 80 nm in x, y and 15 nm in z. The three images were taken successively, with the vibration induced at 113 Hz. To verify that the AC signal follows Eq. (4), we calculated the partial derivatives of the DC response shown in Fig. 1(b), with respect to the different axis. The results, shown in Figs. 1(f)–1(h), are qualitatively similar to the AC data, showing that Eq. (4) is indeed satisfied.

To test the sensitivity of the method, we fabricated a conducting steel wire (1 μm wide and 70 nm thick). When a current is applied through the wire, it generates a magnetic field around it, which we detect with the SQUID. The magnetic field is related to the current as described by the Biot-Savart's law: consider a one-dimensional wire oriented along the y axis, carrying a current I. The z-component of the magnetic field recorded along the x-direction, at a height z above the wire is given by

$$B_z(x) = \frac{\mu_0 I}{4\pi}\frac{x}{x^2+z^2}, \quad (6)$$

where μ_0 is the vacuum permeability. Both the field and its gradient are proportional to the applied current. This allows us to control the signal to noise ratio in both the vibration and DC images, so that the signal is reduced by the same factor in both cases.

Figure 2(a) shows the noise spectral density of our sensor. The spectrum is measured by recording the magnetic signal as a function of time for 50 s, at a rate of 20 kHz, and then calculating the Fourier transform of the data. The sensitivity at low frequencies (1 Hz) is two orders of magnitude lower than the sensitivity at 113 Hz. The spectral noise density shown here is representative of our closed-cycle system. The spectrum is reproducible when measured at different times during a single experiment and between different experiments involving the same sensor. The performance is mostly limited by our system's electronics and wiring, and varies between systems. Furthermore, the noise floor (>100 Hz) we report is comparable to reports by Huber *et al.*[9] and Kirtley *et al.*,[11] while the low frequency noise of the closed cycle system is higher.[13] The noise floor improves at lower operating temperatures.[9] Figures 2(b)–2(e) show the DC and AC responses of the sample, recorded by the SQUID, for two applied DC currents. While the DC signal from a current of 10 nA is below the noise of our sensor, it is still easily observed through the response to the vibration. This confirms the superior sensitivity of this method.

Having established the enhanced sensitivity over the DC measurement, we turn to study the efficiency of this method, for different excitation frequencies. According to Eq. (5), the

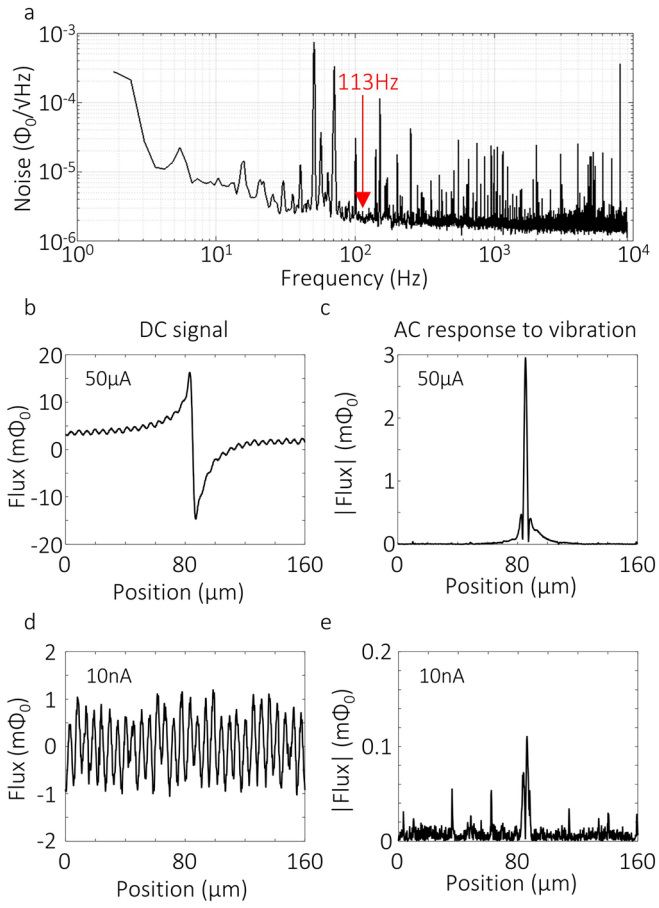

FIG. 2. Sensitivity enhancement by vibrations. (a) The SQUID's noise power spectrum shows a significant 1/f noise in low frequencies. The smallest detectable flux at 1 Hz is $2.8 \times 10^{-4}\Phi_0$, while the smallest detectable flux at 113 Hz (where the vibrations were induced, indicated by a red arrow) is $2.25 \times 10^{-6}\Phi_0$. (b) Magnetic flux generated by a long wire (positioned at $x = 85$ μm) carrying a DC current of 50 μA. The signal is obtained by moving the SQUID across the profile of the wire and follows equation 5 (up to a convolution with the sensor's point spread function). (c) The absolute value of the AC response to a vibration induced along the measured profile, with an amplitude of 1 μm at 113 Hz. The signal shows a peak at $x = 85$ μm, where the wire is placed. (d) and (e) Same as (b) and (c) with a lower current, 10 nA, chosen so that the DC signal would fall below our noise level. Other measurement parameters that determine the sensitivity (such as averaging time) were kept as in (b) and (c). While the DC signal was below our sensitivity, the AC response still shows a peak at $x = 85$ μm, that is distinguished from the noise. Additional peaks in e are noise at random frequencies. The data in panel (a) were recorded at a sensor-sample distance of 2 μm, while the data in panels (b)–(e) were recorded at a constant scan height of 1.25 μm. The noise spectrum in panel (a) is independent of height for frequencies larger than 2 Hz.

signal resulting from the vibration should be proportional to the vibration amplitude. In principle, this proportionality should be frequency-independent, but the piezoelectric components used for scanning, as well as the overall configuration of the scanner, might affect the coupling between the piezo elements and the sample.

To study this proportionality constant, we position our SQUID at a single point and record the magnetic signal as a function of time. We then calculate the noise spectral density. We vibrate the x-piezo at a specified frequency and record the noise spectra for different vibration amplitudes. Representative results for $f = 29$ Hz are shown in Fig. 3(a). When the sample vibrates, we observe a peak in the power spectrum, located at the vibration frequency. The intensity of

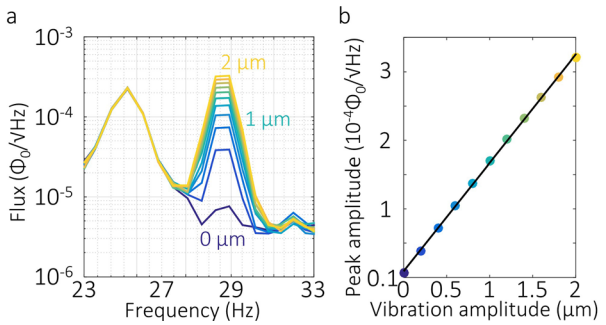

FIG. 3. Amplitude dependence of the response to vibration. (a) Segments of the noise spectral density, in the frequency range of 23 Hz–33 Hz (full spectra are similar to the one shown in Fig. 2(a). Each spectrum corresponds to a measurement recorded while the x-piezo was vibrating at 29 Hz, with different vibration amplitudes, ranging from 0 μm (no vibration) (blue) to 2 μm (yellow). A peak develops around the excitation frequency when the sample vibrates and its intensity increases with the vibration intensity. In other frequencies, the noise is independent of the vibration. (b) Noise density at 29 Hz plotted against the amplitude of the vibration (dots) shows that the response is linear in the vibration amplitude. The solid line is a linear fit to the data, with a slope of $1.58 \times 10^{-4}\Phi_0/\sqrt{\text{Hz}}/\mu$m.

this peak increases as we increase the intensity of the vibration.

The response is ~3 Hz wide and at frequencies further than that width, the noise is independent of the vibration amplitude. For example, Fig. 3(a) also shows a large peak at 25 Hz, which corresponds to the operating frequency of the cooling system's compressor. This peak does not show any dependence on the vibration intensity.

Figure 3(b) shows the amplitude of the peak as a function of the vibration intensity, verifying that the response is linear in the intensity regime we studied. We can extract the slope of this curve, which is a measure of the effectiveness of our method at that frequency.

Figure 4 shows slopes extracted in the same way for different vibration frequencies. We observe frequency bands where the response to vibrations is strongly suppressed, as

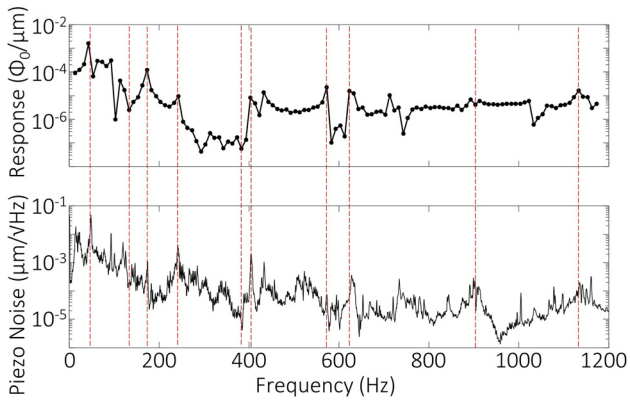

FIG. 4. Frequency dependence of the response. (top) Change in the magnetic signal recorded by the SQUID due to change in the vibration amplitude (as shown in Fig. 3) as a function of frequency, in the range of 13 Hz–1200 Hz. The response spectrum is non-monotonic and exhibits regions of suppressed response (for example, 250 Hz–400 Hz), as well as isolated peaks and dips. (bottom) Noise spectral density of the x-piezo element, measured by recording the voltage drop on the piezo as a function of time and calculating the Fourier transform of the data. In large parts of the spectrum, the piezo noise curve behaves similarly to the magnetic response to vibrations. Some examples are highlighted by the red dashed lines.

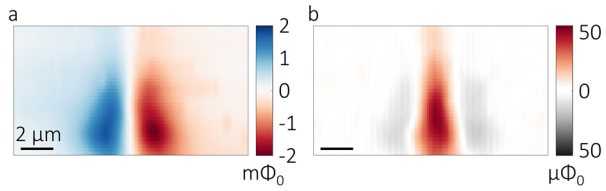

FIG. 5. Response to vibrations of a point dipole. (a) The DC magnetic flux generated by a nano-magnet. (b) The AC response to a vibration of 40 nm in the horizontal axis.

well as narrow peaks of enhanced response. To understand this unexpected response, we compare it to the noise spectrum of the piezo itself. The two spectra look remarkably similar, supporting the scenario where the piezoelectric elements influence the coupling of vibrations to the system. This suggests that each piezo based system would have a set of more favorable frequencies for optimal performance. Indeed, we observed similar behavior using another piezoelectric scanner, with the same design. While the magnetic response was not monotonic and roughly followed the piezo noise, specific frequency ranges varied between the different scanners. This suggests that the details of the scanner's structure influence the magnetic response. While the data show compelling evidence to support this scenario, further work is required to give a full account of the surprising frequency response we observe. Optimizing the design of the scanner can enable elimination of vibrations in specific frequencies and improve the effectiveness of the vibration induced imaging method in other frequencies.

Finally, we turn to discuss the applicability of our method. In the realm of magnetic imaging, we demonstrated the technique on point-like objects and current sources. Small magnetic moments can also be imaged using this method. To demonstrate this, we imaged the DC magnetic field generated by a nano-magnetic object and the AC response to a 40 nm vibration applied to the x direction. Figure 5(a) shows the DC magnetic flux image generated by the magnetic moment. The dipole can be modeled by two, slightly shifted vortices [Fig. 1(b)], with opposite signs. When applying a vibration to the vertical axis, the vortices that "compose" the dipole turn into two dipoles [Fig. 1(c)], with opposite moments. Since the two dipoles have opposite directions, their combined signal is large at the position of the original moment. This result is shown in Fig. 5(b), where the response to vibrations was imaged.

To conclude, we developed a method for utilizing vibrations in a scanning system to enhance the sensitivity to DC signals. We demonstrated this method using a scanning SQUID microscope on several magnetic field sources and showed that the sensitivity is increased, compared to DC imaging. This technique can be readily applied to a wide range of imaging systems, where high sensitivity to DC field sources is required.

This research was supported by the European Research Council Grant No. ERC-2014-STG-639792, the Israeli Science Foundation Grant No. ISF-1281/17, COST Action CA16218, and the QuantERA ERA-NET Cofund in Quantum Technologies (Project No. 731473).

[1]F. Gömöry, "Characterization of high-temperature superconductors by AC susceptibility measurements," Supercond. Sci. Technol. **10**, 523 (1997).
[2]S. Pilla, J. A. Hamida, and N. S. Sullivan, "Very high sensitivity ac capacitance bridge for the dielectric study of molecular solids at low temperatures," Rev. Sci. Instrum. **70**, 4055–4058 (1999).
[3]S. Foner, "Versatile and sensitive vibrating-sample magnetometer," Rev. Sci. Instrum. **30**, 548–557 (1959).
[4]Q. Zhong, D. Inniss, K. Kjoller, and V. B. Elings, "Fractured polymer/silica fiber surface studied by tapping mode atomic force microscopy," Surf. Sci. Lett. **290**, L688–L692 (1993).
[5]T. R. Albrecht, P. Grütter, D. Horne, and D. Rugar, "Frequency modulation detection using high-Q cantilevers for enhanced force microscope sensitivity," J. Appl. Phys. **69**, 668–673 (1991).
[6]B. D. Josephson, "Possible new effects in superconductive tunnelling," Phys. Lett. **1**, 251–253 (1962).
[7]J. Clarke and A. I. Braginski, *The SQUID Handbook: Fundamentals and Technology of SQUIDs and SQUID Systems* (Wiley–VCH, New York, 2004), Vol. I.
[8]J. R. Kirtley, M. B. Ketchen, K. G. Stawiasz, J. Z. Sun, W. J. Gallagher, S. H. Blanton, and S. J. Wind, "High-resolution scanning SQUID microscope," Appl. Phys. Lett. **66**, 1138–1140 (1995).
[9]M. E. Huber, N. C. Koshnick, H. Bluhm, L. J. Archuleta, T. Azua, P. G. Björnsson, B. W. Gardner, S. T. Halloran, E. A. Lucero, and K. A. Moler, "Gradiometric micro-SQUID susceptometer for scanning measurements of mesoscopic samples," Rev. Sci. Instrum. **79**, 53704 (2008).
[10]N. C. Koshnick, M. E. Huber, J. A. Bert, C. W. Hicks, J. Large, H. Edwards, and K. A. Moler, "A terraced scanning super conducting quantum interference device susceptometer with submicron pickup loops," Appl. Phys. Lett. **93**, 243101 (2008).
[11]J. R. Kirtley, L. Paulius, A. J. Rosenberg, J. C. Palmstrom, C. M. Holland, E. M. Spanton, D. Schiessl, C. L. Jermain, J. Gibbons, Y.-K.-K. Fung, M. E. Huber, D. C. Ralph, M. B. Ketchen, G. W. Gibson, Jr., and K. A. Moler, "Scanning SQUID susceptometers with sub-micron spatial resolution," Rev. Sci. Instrum. **87**, 093702 (2016).
[12]J. Siegel, J. Witt, N. Venturi, and S. Field, "Compact large-range cryogenic scanner," Rev. Sci. Instrum. **66**, 2520–2523 (1995).
[13]N. Vardi, Y. Shperber, E. Persky, S. Wissberg, M. Huber, and B. Kalisky, "Cryogen free scanning SQUID microscopy" (unpublished).
[14]D. Schiessl, J. R. Kirtley, L. Paulius, A. J. Rosenberg, J. C. Palmstrom, R. R. Ullah, C. M. Holland, Y.-K.-K. Fung, M. B. Ketchen, G. W. Gibson, and K. A. Moler, "Determining the vibrations between sensor and sample in SQUID microscopy," Appl. Phys. Lett. **109**, 232601 (2016).